



Research article

Modelling the transmission and control of COVID-19 in Yangzhou city with the implementation of Zero-COVID policy

Juan Li¹, Wendi Bao², Xianghong Zhang³, Yongzhong Song⁴, Zhigui Lin⁵ and Huaiping Zhu^{6,*}

¹ School of Computer Science and Technology (School of Artificial Intelligence), Zhejiang Sci-Tech University, Hangzhou 310018, China

² College of Science, China University of Petroleum, Qingdao 266580, China

³ School of Mathematics and Statistics, Southwest University, Chongqing 400715, China

⁴ Jiangsu Key Laboratory for NSLSCS, Institute of Mathematics School of Mathematics Science Nanjing Normal University, Nanjing 210023, China

⁵ School of Mathematical Science, Yangzhou University, Yangzhou 225002, China

⁶ LAMPS and Center for Diseases Modeling (CDM), Department of Mathematics and Statistics, York University, Toronto M3J 1P3, ON, Canada

* **Correspondence:** Email: huaiping@yorku.ca; Tel: +4167362100; Ext: 66095.

Abstract: In the fight against the COVID-19 pandemic, China has long adhered to the “Dynamic Zero COVID-19” strategy till the end of 2022. To understand the mechanism of this strategy, we used the case of the Yangzhou summer outbreak in 2021 and a multi-stage dynamical model incorporating city-wide and key area testing-trace-isolation (TTI) strategies. We defined two time-varying indexes for measuring the disease transmission risk and the public health prevention and control force, respectively, which allowed us to explore the mechanisms of TTI policies. Integrating with the historical data and literature parameter values, we first estimated the parameters and then quantified the relevant indexes over time. The findings showed that multiple rounds of rapid testing were one of the critical measures to overcome the outbreak in Yangzhou within one month. In addition, we compared the impact of the duration of the free transmission stage, tracking rate, testing interval and precise division of key areas on the epidemiological indicators, including the final sizes of infections and isolations, peak value, peak arrival time and epidemic duration and the minimum round of testing. Our results suggest that the early detection of the epidemic, an improved efficiency of tracking, and a reduced duration of each test play a positive role in restraining COVID-19; however, a considerable investment of resources was essential to achieve a significant effect quickly.

Keywords: COVID-19; dynamic Zero strategy; a multi-stage dynamical modeling; city-wide test-trace-isolation (CTTI); key area test-trace-isolation (KTTI); public health prevention and control force

1. Introduction

Since the first outbreak of COVID-19, human health has been continuously endangered. As of May 29th, 2023, the Center for Systems Science and Engineering (CSSE) at Johns Hopkins University reported 676,609,955 of lab-confirmed cases with 6,881,955 deaths, and 4,035,254 new cases, including 28,018 deaths within the last 28 days [1]. Over the past three years, SARS-COV-2 concern variants (VOC) have continued to evolve in countries or regions with a high virus transmission and low vaccine coverage [2]. The transmission power of the virus has increased from Alpha to Delta and then to Omicron; now, the transmission intensity of the VOCs with a basic reproduction number R_0 (Delta: 3.2–8, Omicron: 3.47–10) is almost 3–5 times that of the ancestral strain (2.5–2.79) [3,4]. Although the pathogenicity of the new mutant strain has been weakened, the social and economic impact caused by the epidemic continues due to its strong infectivity, fast transmission, high concealment and a large number of infected people [5,6]. Finally, on May 5, 2023, the World Health Organization (WHO) declared an end to the public health COVID-19 emergency of international concern [7]. However, that does not mean that COVID-19 is over as a global health threat and waves of endemics continues.

During the past three years, countries have adopted different public health perspectives to fight the raging epidemic worldwide. So far, these countries have two main strategies. One strategy includes an elimination strategy (“Zero COVID-19” strategy) that aims to eradicate all cases whenever a fresh outbreak occurs [8,9]. China is the most representative [10]. Singapore, Australia, New Zealand, Iceland, Japan, South Korea and other countries have also implemented the elimination strategy. Another strategy includes a mitigation strategy (“coexistence with the virus” strategy) that aims to reduce cases to overwhelm healthcare systems by increasing the activity in a stepwise and targeted way [8,9]. The United States is the most representative and most Western country to adopt this method.

Elimination and mitigation sparked a heated debate on social media. With increasing vaccination numbers and economic pressures, some countries, including South Korea, Italy, Australia and New Zealand, have begun to lift their original strategies, and just maintained a loose testing target to prevent the medical system and intensive care units (ICUs) from becoming overwhelmed. Unfortunately, their situation is not an optimistic exception. Taking South Korea as an example, since the vaccination rate reached 70%, the government launched a mitigation strategy on Nov. 1, 2021. However, in less than ten days, the epidemic in South Korea returned to a terrible situation, with the number of locally critical patients quickly surging to a record high. What’s worse, the previous anti-epidemic achievements of South Korea are coming to naught [11]. It is a dilemma for many countries regarding which anti-epidemic path, either elimination or mitigation, should be committed.

In response to the local rebounds and sporadic cases of COVID-19, the Chinese government consistently adhered to the elimination strategy and had successfully eliminated each outbreak whenever it occurred [12,13]. Once an indigenous case was found, the public health department of China would immediately start joint prevention and control measures, increase medical staff, material and financial resources, implement intervention measures such as tracking, isolation, lockdown and city-wide testing, timely block the transmission chain and quickly curbed the epidemic [14]. Any

specific actions that can effectively control the infection source, cut off the transmission route and protect vulnerable people will contribute to prevent and control the epidemic. Thus, the above three basic principles should be strictly followed while considering the characteristics of the outbreak and epidemic in different periods. The NHCC (National Health Commission of China) has issued nine editions of COVID-19 diagnosis and treatment protocols, striving for an efficient and precise prevention and control as much as possible and high cooperation with the public, to improve the prevention and control ability, effectively curb the spread of the epidemic, and achieve zero COVID-19 [15].

China has a huge population; once it embraces specific “open-up” strategies, the impact on the medical system will be devastating. Even in the case of a highly underestimated outbreak, it is estimated that the number of new confirmed cases in China would likely rise to hundreds of thousands per day, including more than 10,000 severe cases [16]. China did not hesitate to carry out multiple rounds of population-wide nucleic acid testing (NAT) for each epidemic. Due to the existence of the window period (the window period refers to the period from the pathogen entering the human body to being detected through specific detection techniques) and the omission of sampling and detection, it is not easy to find all infected people or sources of infection at once. The implementation of multiple rounds of city-wide tracing-testing-isolation (CTTI) strategy accurately detects pathogens, more accurately performs prevention and control, locates infected people and cuts off the virus transmission chain [10]. However, strict epidemic prevention and control had not only brought many inconveniences to people’s daily life, but also had a significant impact on the social economy [9]. The epidemic prevention and control strategies are not static, and will change according to the domestic and foreign situations. Therefore, it is important to fully understand the implementation mechanism of these Zero-COVID prevention and control strategies, evaluate the effectiveness of intervention measures immediately, optimize and analyze the impacts of different degrees of strategy adjustment on the occurrence and evolution of the epidemic.

To understand the transmission and mechanism of different control methods, dynamic modeling has played a more critical role. To date, this approach has been widely used in assessing control measures such as tracking, testing and/or isolation. With an extended susceptible-exposed-infectious-removed (SEIR) model, Tang et al. [17] evaluated the effectiveness of quarantine and isolation in determining the trend of China’s COVID-19 epidemic in the final phase in early 2020. Hou et al. [18] devised a well-mixed SEIR compartmental model to describe the dynamics of the COVID-19 epidemic in Wuhan City and to quantify the change in the potential peak number of COVID-19 infections and the time of the peak infection concerning the interventions such as quarantine and isolation. Based on a susceptible-exposed-infectious-quarantined-removed (SEIQR) compartmental model, Shimizu et al. [19] explored possible scenarios for decreasing COVID-19 incidence in Okinawa by combining population-wide screening and/or social distancing policy. Integrating anonymized, delocalized mobility data with census and demographic data, Aleta et al. [20] built a detailed agent-based model of SARS-CoV-2 transmission in the Boston metropolitan area to analyze the influence of testing, contact-tracking and household quarantine levels on the healthcare system and economic activities. Colbourn et al. [21] estimated the impact of different testing-trace-isolation (TTI) strategies with a deterministic mathematic model of SARS-CoV-2 transmission in the UK. Kucharski et al. [22] simulated the effect of a range of different testing, isolation, tracking, and physical distancing scenarios on the epidemic in the UK by a model of individual-level transmissions stratified by setting (household, work, school, or other). Contreras et al. [23] exploited a semi-analytical model to expound that TTI alone is insufficient to contain an otherwise unhindered

spread of SARS-CoV-2 if comprehensive measures are not taken. However, previous models did not reflect the essence of China's current "Dynamic Zero COVID-19" strategy. It is necessary to develop a dynamical model containing multiple rounds of city-wide TTI (CTTI) strategies to describe the epidemic control mechanism and evaluate the effectiveness of the "Dynamic Zero COVID-19" strategy based on the actual situation in China.

The Yangzhou outbreak is typical of China's many campaigns against COVID-19. Taking Yangzhou as an example, this paper will use a mathematical model to study the mechanism of China's "Dynamic Zero COVID-19" strategy. Based on the actual and historical confirmed case data in Yangzhou from July 21 to Aug. 26, we will explore the model inversion to obtain unknown parameters. Then, we will compare and analyze the epidemiological indicators of the epidemic under different scenarios through simulations, including different control modes (elimination mode, lying flat mode with "Coexistence with the virus" and the negative mode with only detecting without tracking and isolation), duration of free transmission phase, tracking rate, testing interval, etc., and discuss the minimum testing times required to end the outbreak. Additionally, we will define two time-dependent indicators to describe the transmission risk and public health prevention and control efforts throughout the outbreak. This study aims to provide a theoretical insight and reference for the scientific prevention and control of current global COVID-19 cases and possible emerging infectious diseases in the future.

2. Data and modelling

2.1. Data sources

The data used in this study were obtained from the official websites of the Yangzhou Commission of Health [24] and the Chinese website PAPERS [25]. First, for modeling, we systemically reviewed the occurrence and development of the epidemic in Yangzhou. As shown in Figure 1, due to an infectious older woman leaving the epidemic area and entering Yangzhou without authorization on July 21, 2021, an epidemic broke out in the main urban area of Yangzhou, a city in Jiangsu province in China. On July 28, after she was the first confirmed case, the Yangzhou Municipal Government and the disease control department quickly and decisively decided to announce the closure of the city on July 31. The daily lives of 1.7 million people have been suspended due to the outbreak. The main urban area adopted a strict TTI elimination strategy. Seven rounds of CTTI were carried out on July 28, Aug. 01, Aug. 05, Aug. 07, Aug. 09, Aug. 11 and Aug. 12, respectively. Since Aug. 14, Yangzhou has intensively carried out daily key areas TTI (KTTI) in the main urban area. As of Sep. 01, Yangzhou has accurately carried out 18 rounds of NAT for key populations in key areas, with a total of 23.55 million people being sampled and tested. Until Sep. 09, Yangzhou announced that all cases had been eradicated and the lockdown was fully lifted. This outbreak was caused by the Delta virus, and had characteristics of untimely discovery, aggregation infection, divergent transmission, strong infectivity and fast transmission, resulting in a total of 572 confirmed infections, with 237 from isolation zones and 335 from communities and fever clinics. Second, we collated three datasets by reporting date, including daily confirmed cases in and outside the isolation zone (IZ) from July 21 to Aug. 31, 2021, as well as partial discrete data on the primary and secondary contacts from July 30 to Aug. 10, to calibrate the models and estimate some uncertain parameters.

2.2. A multi-stage model for CTTI eliminating process

Based on the epidemiological characteristics of individuals, the clinical progression of COVID-19, and the intervention strategies adopted, we extend the basic SEIR compartmental model to consider complete isolation followed by a TTI policy to describe the spread dynamics and control process of COVID-19 in Yangzhou city.

Considering Yangzhou, an area with a total population size of N_0 , we divided all individuals without isolation management into four groups: susceptible (S) (vulnerable to infection), exposed (E) (latent individuals, not infectious and negative if tested), infectious (I) (including asymptomatic, prodromal infected and symptomatic infected, capable of spreading COVID-19) and removed (R) (recovery and death). In particular, we consider a special compartment representing an IZ in which people have to undergo a 14-day observation collectively and then a 7-day at home [15], with all individuals massively isolated through the repeated TTIs coming from the four groups: susceptible (Q_S), exposed (Q_E), undiagnosed but infectious (Q_I), and confirmed (I_C), and denote the total number of individuals in this compartment as $Q(t)$, $Q(t) = Q_S(t) + Q_E(t) + Q_I(t) + I_C(t)$.

There are several main assumptions:

- Only infectious individuals (I) can test positive with $\theta(i)$ test accuracy for (I) in round i , all of which can be detected after multiple rounds of testing.
- Part of the susceptible (S), infectious (I) and exposed (E) groups may be quarantined or asked to isolate through contact tracing.
- None of the individuals in Q can promote the spread of the epidemic.
- Secondary infection is not considered.
- Whether it's for the whole region or key areas, we assume that no infected person will be missed in each round of tests.

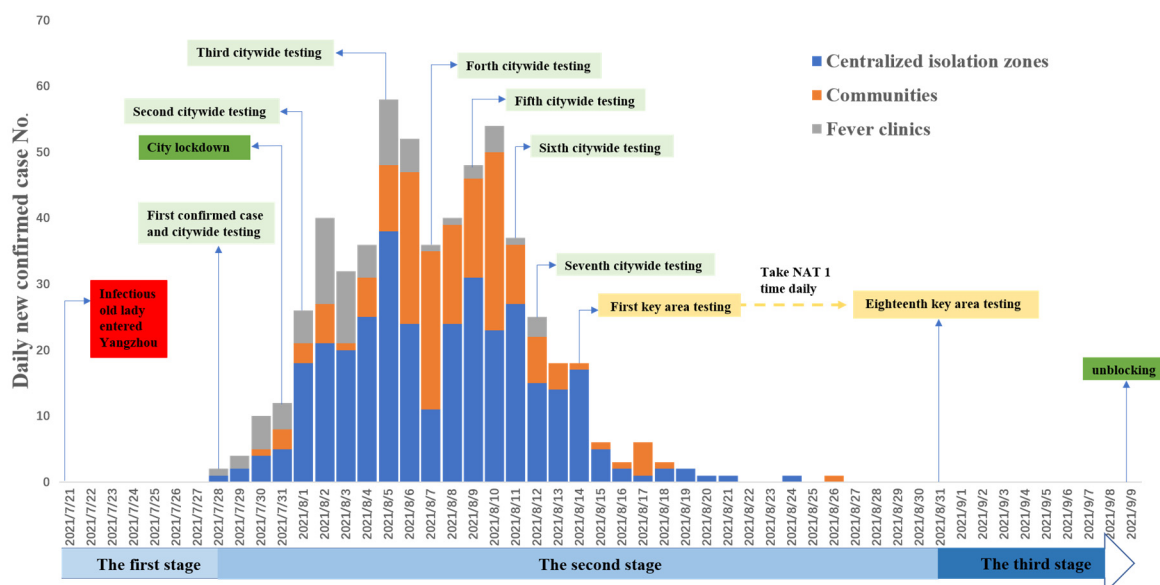


Figure 1. Temporal distributions of the confirmed cases and the adopted intervention strategies in Yangzhou. Data source from [24].

To establish a dynamical model more in line with the development and control of the outbreak in Yangzhou, we focus on some key time points by reviewing the epidemic reporting data in Yangzhou (see Figure 1). We denote the date when the infected older woman entered Yangzhou by T_0 (July 21), the date when the city-wide testing started by T_1 (July 28), the date when the multiple rounds of TTIs stopped by T_2 (Aug. 15), and the date when the epidemic situation was comprehensively curbed by T_3 (Aug. 26).

Then, we study the elimination dynamics of the Yangzhou epidemic in three stages:

- (i) Free transmission stage ($T_0 \rightarrow T_1$): free transmission happens until the first case is confirmed on the day $t = T_1$.
- (ii) TTI eliminating stage ($T_1 \rightarrow T_2$): multiple rounds of TTIs are carried out till no more individuals go to Q for τ (a latent period) consecutive days.
- (iii) Clearing stage ($T_2 \rightarrow T_3$): no new case appears till the city is fully opening again.

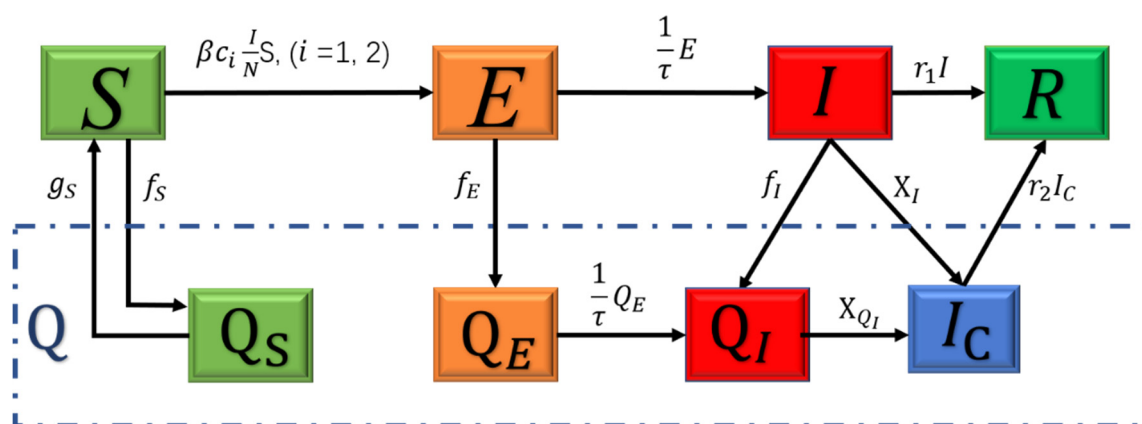


Figure 2. Flow diagram on the dynamical transmission of COVID-19 virus among humans in Yangzhou city. The rectangles of different colors represent the compartments of different people groups. Solid lines show the direction where each compartment proceeds, dashed rectangle represents the isolation point. Note: without all parts in the dashed rectangle and the class R , the flowchart shows the dynamical transmission of the COVID-19 virus in the first stage.

Then, we construct the following two-stage model, emphasizing the role of the “Dynamic Zero COVID-19” policy in clearing the epidemic in Yangzhou. See the flow diagram of the model in Figure 2.

For the free transmission stage ($T_0 < t < T_1$), we have a simple SEIR model:

$$\begin{cases} \frac{dS}{dt} = -\beta c_1 I \frac{S}{N}, \\ \frac{dE}{dt} = \beta c_1 I \frac{S}{N} - \frac{1}{\tau} E, \\ \frac{dI}{dt} = \frac{1}{\tau} E - r_1 I, \\ \frac{dR}{dt} = r_1 I. \end{cases} \quad (\text{Model I})$$

For the eliminating stage ($T_{i,1} \leq t < T_{i,k_i} \leq T_2, i = 1, 2, 3, \dots, n$), Model I becomes the following:

$$\left\{ \begin{array}{l} \frac{dS}{dt} = -\beta c_2 I \frac{S}{N} - f_S(X_I, X_{Q_I}, T, c_2, c_S) + f_S(t - \tau_Q), \\ \frac{dE}{dt} = \beta c_2 I \frac{S}{N} - \frac{1}{\tau} E - f_E, \\ \frac{dI}{dt} = \frac{1}{\tau} E - f_I(X_I, X_{Q_I}, T, c_2, c_S) - X_I - r_1 I, \\ \frac{dQ_S}{dt} = f_S(X_I, X_{Q_I}, T, c_2, c_S) - f_S(t - \tau_Q), \\ \frac{dQ_E}{dt} = f_E(X_I, X_{Q_I}, T, c_2, c_S) - \frac{1}{\tau} Q_E, \\ \frac{dQ_I}{dt} = f_I + \frac{1}{\tau} Q_E - X_{Q_I}, \\ \frac{dI_C}{dt} = X_I + X_{Q_I} - r_2 I_C, \\ \frac{dR}{dt} = r_2 I_C + r_1 I. \end{array} \right. \quad (\text{Model II})$$

In the model, the subscripts i and k of T_{i,k_i} represent the i th-round CTTI and the number of days required for the i -round testing, respectively, where $N(t) = S(t) + E(t) + I(t) + R(t)$. All variables and parameters in models are summarized in Table 1 and the detailed design processes of f_S , f_E , f_I , g_S , X_I and X_{Q_I} are shown as follows.

2.2.1. Estimate the daily number of confirmed cases $X = X_I(t) + X_{Q_I}(t)$

The accuracy rate of NAT for COVID-19 is relatively high. In general, the accuracy rate of a single test is about 80%, and the accuracy rate of a double test is more [26]. Then, we assume that the accuracy rate θ of repeated i testing should satisfy the following:

- i. $\theta(i)$ is continuously differentiable for $i \in R^+$,
- ii. $\theta(0) = 0$,
- iii. $\lim_{i \rightarrow \infty} \theta(i) = 1$,
- iv. $\frac{d\theta(i)}{di} > 0$ for any i .

To put it simply, in this study we can take $\theta(i) = \frac{i}{i_0+i}$, i_0 as a constant.

With the development of the epidemic, Yangzhou began to complete city-wide testing, and then focused on key-area testing. Whether it is a whole area or a key area, we assume that all infected people are on the testing list in each round of testing. The second phase will stop if the total quarantined number $Q(t)$ remains unchanged for τ consecutive days. We assume that the size of the total population tested outside the IZ on day t is $\mu_1(N_0 - Q(t))$, where μ_1 is the proportion of the tested individuals in the total non-isolated individuals, with $\mu_1 = 1$ for city-wide testing and $\mu_1 < 1$ for key-area testing. The whole process of testing is assumed to be finished within k_i day(s). Therefore, the daily number of individuals tested outside the IZ is approximately $\frac{\mu_1(N_0 - Q(t))}{k_i}$.

The average number of infectious individuals detected outside the IZ per day is $\frac{\mu_1(N_0 - Q(t))}{k_i}$.

$\frac{I(t)}{\mu_1(N_0 - Q(t))} = \frac{1}{k_i} I(t)$. The average daily number of confirmed cases outside the IZ for i -round testing is

$$\theta(i) \cdot \frac{1}{k_i} I(t),$$

i.e., the daily number of newly confirmed cases outside IZ on day t is

$$X_I(t) = \theta(i) \frac{1}{k_i} I(t), T_{i,1} \leq t < T_{i,k_i} \quad (i = 1, 2, \dots, n).$$

Due to the particularity of the individuals in IZ, we assume that everyone who should be tested will be detected in time and done within one day. Let $I_C(t)$ be the total confirmed cases in IZ at time t , the total population size tested in IZ on day t is $(Q(t) - I_C(t))$. In addition, the daily number of new confirmed cases in IZ on day t is given by the following:

$$X_{Q_I}(t) = \theta(i) \cdot (Q(t) - I_C(t)) \cdot \frac{Q_I(t)}{Q(t) - I_C(t)} = \theta(i) Q_I(t), T_{i,1} \leq t < T_{i,k} \quad (i = 1, 2, \dots, n).$$

Therefore, the daily total number of newly confirmed cases on day t is as follows:

$$X(t) = X_I(t) + X_{Q_I}(t).$$

2.2.2. Estimate the daily number of isolated individuals (susceptible f_S , exposed f_E and infectious f_I)

Let c_2 and c_s be the average primary contact number per confirmed case and the average non-primary contacts number per primary contact before being isolated per day, respectively. The average number of primary contacts and secondary contacts per day of all confirmed cases are $c_2 X(t)$ and $c_s c_2 X(t)$, respectively.

Let T be the average time from infectious to confirmed of a person, then the confirmed cases on day t can only infect others during the period from $t - T$ to t , and β be the effective rate of susceptible one contacting the infectious individual to be infected successfully. For any $s (s \in (t - T, t))$, we ignore the fund process of the primary and secondary contacts in the form of mathematics based on the conceptual diagram Figure 3.

2.2.3. Primary and secondary contacts

Primary contacts are those who have direct and close contact with a confirmed case. Primary contacts may be susceptible (S), exposed (E), or infectious (I). If the confirmed case comes into contact with a susceptible person, the susceptible person is likely to be infected with an average infection efficiency β . If an exposed person is contacted by confirmed cases, then the exposed person may still be in the exposed state or becomes infected at that time with a transfer rate $\frac{1}{\tau}$. If an infectious person is contacted, he/she will still be in the infectious state. It is noteworthy that the susceptible primary contact may be infected by a secondary contact who has been infectious, see the conceptual diagram in Figure 3. Then, we can derive the number of primary contacts who are susceptible at the time s is

$$Y_{S1}(s) = (1 - \beta) \cdot c_2 X(t) \cdot \frac{S(s)}{N(s)} \cdot \left(1 - \beta \frac{I(s)}{N(s)}\right),$$

where $c_2 X(t) \cdot \frac{S(s)}{N(s)}$ is the number of susceptible persons contacted by the confirmed cases at time s ; $(1 - \beta) \cdot c_2 X(t) \cdot \frac{S(s)}{N(s)}$ is the number of susceptible persons contacted and not successfully infected by the confirmed cases at the time s ; and $(1 - \beta) \cdot c_2 X(t) \cdot \frac{S(s)}{N(s)} \cdot \beta \frac{I(s)}{N(s)}$ is the number of susceptible persons successfully infected by secondary close contacts.

Similarly, the number of primary contacts who are exposed at the time s is

$$Y_{E1}(s) = \left(1 - \frac{1}{\tau}\right) \cdot c_2 X(t) \cdot \frac{E(s)}{N(s)} + \beta \cdot c_2 X(t) \cdot \frac{S(s)}{N(s)} + (1 - \beta) \cdot c_2 X(t) \cdot \frac{S(s)}{N(s)} \cdot \beta \frac{I(s)}{N(s)}$$

and the number of primary contacts who are infectious at the time s is

$$Y_{I1}(s) = c_2 X(t) \cdot \frac{I(s)}{N(s)} + \frac{1}{\tau} \cdot c_2 X(t) \cdot \frac{E(s)}{N(s)}$$

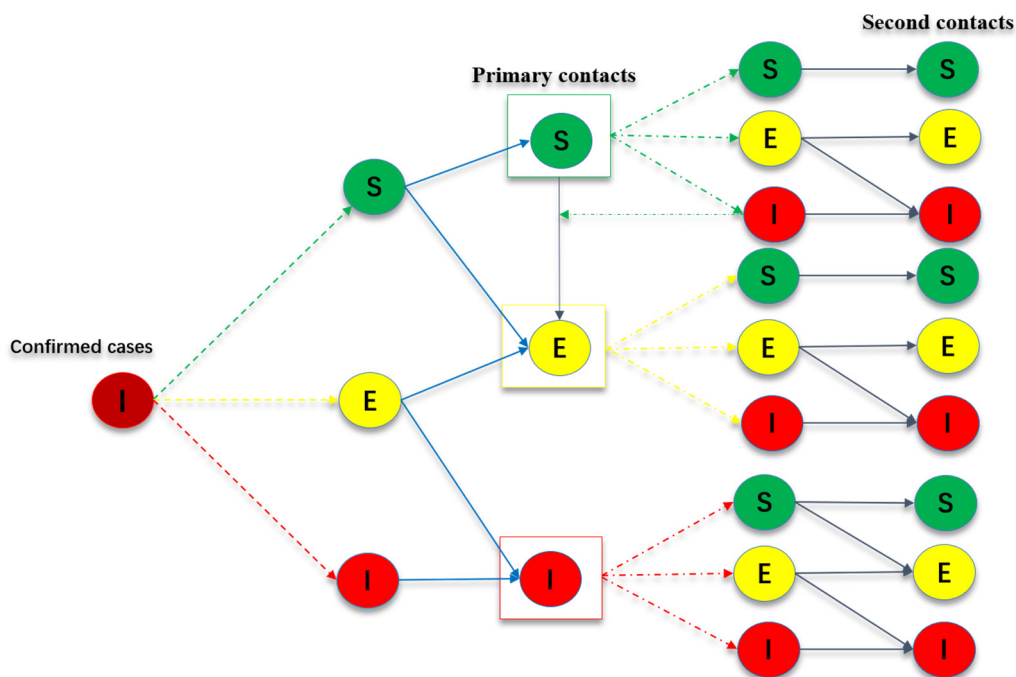


Figure 3. Conceptual diagram of primary and second contacts with confirmed cases. Solid lines denote the changes in compartments, dashed lines indicate the contact among people in different compartments.

For the secondary contacts, we employ a derivation process similar to that of the primary contacts. Then, we have the number of new secondary contacts who are susceptible at time s as follows:

$$Y_{S2}(s) = c_s Y_{S1} \frac{S(s)}{N(s)} + c_s Y_{E1} \frac{S(s)}{N(s)} + c_s Y_{I1} \frac{S(s)}{N(s)} (1 - \beta).$$

The number of new secondary contacts who are exposed at time s is as follows:

$$Y_{E2}(s) = \left(1 - \frac{1}{\tau}\right) c_s Y_{S1} \frac{E(s)}{N(s)} + \left(1 - \frac{1}{\tau}\right) c_s Y_{E1} \frac{E(s)}{N(s)} + \left(1 - \frac{1}{\tau}\right) c_s Y_{I1} \frac{E(s)}{N(s)} + c_s Y_{I1} \beta \frac{S(s)}{N(s)}.$$

And the number of new secondary contacts who are infectious at the time s is as follows:

$$Y_{I2}(s) = \frac{1}{\tau} c_s Y_{S1} \frac{E(s)}{N(s)} + \frac{1}{\tau} c_s Y_{E1} \frac{E(s)}{N(s)} + c_s Y_{E1} \frac{I(s)}{N(s)} + c_s Y_{I1} \frac{I(s)}{N(s)} + \frac{1}{\tau} c_s Y_{I1} \frac{E(s)}{N(s)}.$$

Let δ be the tracing efficiency (i.e., the average probability of successful tracking of each contact). According to the above derivation, the total number of susceptible, latent and infectious individuals in Q due to the TTI policy on day t can be expressed as follows:

$$f_S(t) = \delta \sum_{s=t-T}^t (Y_{S1}(s) + Y_{S2}(s)),$$

$$f_E(t) = \delta \sum_{s=t-T}^t (Y_{E1}(s) + Y_{E2}(s)),$$

$$f_I(t) = \delta \sum_{s=t-T}^t (Y_{I1}(s) + Y_{I2}(s)).$$

2.2.4. Estimate the daily number of susceptible persons lifted from isolation

According to the policy mandated by Chinese health authorities, once isolated, even if they have been quarantined for 14 days and tested negative, susceptible persons will still require 7-day health monitoring after being lifted [15]. We assume the duration of the population in Q_S to be observed in τ_Q days. Then, the susceptible people leaving Q_S at time t are those entering Q_S at time $t - \tau_Q$ (i.e., we have $f_S(t - \tau_Q)$).

2.2.5. Initial conditions and stopping TTI criteria

The initial conditions are given as follows:

$$S(T_0) = N_0 - 1, E(T_0) = 0, I(T_0) = 1,$$

$$S(T_{i+1,1}) = S(T_{i,k_i}), E(T_{i+1,1}) = E(T_{i,k_i}), I(T_{i+1,1}) = I(T_{i,k_i}), R(T_{i+1,1}) = R(T_{i,k_i}),$$

$$Q_S(T_{i+1,1}) = Q_S(T_{i,k_i}), Q_E(T_{i+1,1}) = Q_E(T_{i,k_i}), Q_I(T_{i+1,1}) = Q_I(T_{i,k_i}), I_C(T_{i+1,1}) = I_C(T_{i,k_i})$$

with $S(T_{1,1}) = S(T_1)$, $E(T_{1,1}) = E(T_1)$, $I(T_{1,1}) = I(T_1)$, $R(T_{1,1}) = R(T_1)$, $Q_S(T_{1,1}) = Q_E(T_{1,1}) = Q_I(T_{1,1}) = I_C(T_{1,1}) = 0$.

During the implementation of the ‘‘Dynamic Zero-COVID-19’’ policy, there are often multiple rounds of citywide testing. After one round, it is questioned whether another round is needed. Here, we develop the guideline for terminating the CTI. Let $Y(t)$ be the accumulative number of confirmed cases at time t . Then, we have $\frac{dY(t)}{dt} = X$. At the end of each round of testing, check $Y(T_{i,k_i})$:

- (1) The increased value of $Y(T_{i,k_i})$ is zero, i.e., $\frac{dY}{dt} \Big|_{t=T_{i,k_i}} = 0$;
- (2) For $m = 1, 2, \dots, \tau$ (τ denotes the days required for continuous testing of positive patients to be

zero), $Y(T_{i,k_i} + m) = Y(T_{i,k_i})$.

If the above two conditions are satisfied, stop the city-wide TTI; otherwise, perform the next round.

Table 1. Summary on the description of all variables and parameters in the model.

Variable	Meaning	Value	Source
S	Susceptible population outside IZ	$S(T_0) = N_0 - 1$	Data
E	Exposed population outside IZ	$E(T_0) = 0$	Data
I	Infectious population outside IZ	$I(T_0) = 1$	Data
Q_S	Susceptible population in IZ	$Q_S(T_{1,1}) = 0$	Data
Q_E	Exposed population in IZ	$Q_E(T_{1,1}) = 0$	Data
Q_I	Undiagnosed but infectious population in IZs	$Q_I(T_{1,1}) = 0$	Data
I_C	Confirmed cases in IZ	$I_C(T_{1,1}) = 0$	Data
τ	Average latent period	2	[27]
i_0	Adjustable parameter of testing accuracy for I	0.25 [#]	[26]
N_0	Total population size of Yangzhou main city	1,700,000	Data
T_{i1}	Start date of the i -round testing	July 28	Data
T_{ik_i}	End date of the i -round testing	Aug. 14	Data
k_i	Duration for i -round testing	Before Aug. 14: $k_{i=1,2,\dots,7} =$ (4,4,2,2,2,1,2); After Aug. 14: $k_i = 1$	Data
T	Average period per case from infectious to confirmed	4	[28,29]
τ_Q	Duration of the population in Q_S to be isolated	21	[15]
r_1	Recovered rate of infected people outside IZ	Stage I: 1/5 Stage II: 0	[5]
r_2	Recovered rate of infected people from IZ	1/(5+14) ^{##}	[5,15]
τ	Days required for continuous testing after positive patients to be zero	5	Data
Estimated parameter	Meaning	Value (95%CI)	Source
β	Average infection efficiency	9.9837e-02 (9.9302e-02, 10.0409e-02)	MCMC
c_1	Average primary contact number of an infectious one per day in the first stage	1.3980e+01 (1.2972e+01, 1.3996e+01)	MCMC
c_2	Average primary contact number of an infectious one per day in the second stage	Before Aug. 14: 5.6928 (5.3387 5.8005) After Aug. 14: 1.2500 (1.2352, 1.2642)	MCMC

Continued on next page

Estimated parameter	Meaning	Value (95%CI)	Source
c_s	Average number of non-primary contacts per primary contact per day before being isolated	Before Aug. 14: 4.997(4.9404, 5.0077) After Aug. 14: 1.2501(1.2353, 1.2648)	MCMC
δ	Average probability of successful tracing of each contact	2.2393e-01(2.2347e-01, 2.2490e-01)	MCMC

#Derived from $\theta(i)$ with an 80% accuracy rate of one test [26].

##Median length of stay among hospitalized COVID-19 patients is 5, isolation length of patients following hospital discharge is 14 [5,15].

3. Model analysis and control capability indexes

3.1. Theoretical analysis of the model

To better understand the spread-control mechanism by the proposed model, we define the following sequence $P_{i,j}$ by using the numbers of susceptible, exposed and infectious individuals due to the CTTI policy entering Q in the i -round city-wide testing on the day j along with $f_S(t_{i,j})$, $f_E(t_{i,j})$ and $f_I(t_{i,j})$.

Definition: The sequence $P_{i,j} = (f_S(t_{i,j}), f_E(t_{i,j}), f_I(t_{i,j}))$, where $i = 1, 2, 3, \dots, j = 1, 2, 3, \dots, k$, and $f_S(t_{i,j})$, $f_E(t_{i,j})$ and $f_I(t_{i,j})$ are given as follows:

$$f_S(t_{i,j}) = \delta \sum_{s=t_{i,j}-T}^{t_{i,j}} (Y_{S1}(s) + Y_{S2}(s)),$$

$$f_E(t_{i,j}) = \delta \sum_{s=t_{i,j}-T}^{t_{i,j}} (Y_{E1}(s) + Y_{E2}(s)),$$

$$f_I(t_{i,j}) = \delta \sum_{s=t_{i,j}-T}^{t_{i,j}} (Y_{I1}(s) + Y_{I2}(s)).$$

Then, we will summarize the result of the convergence of the model solution in the following theorem.

Theorem 1. If there is a (i, k_i) that satisfies $\frac{dY}{dt} \Big|_{t=T_{i,k_i}} = 0$, and for each $m = 1, 2, \dots, \tau$, $Y(T_{i,k_i} + m) = Y(T_{i,k_i})$, then $P_{i,j} \rightarrow (0,0,0)$ for $t_{i,j} \rightarrow T_{i,k_i} + \tau$, which is equivalent to $(E, I) \rightarrow (0,0)$ and the endemic will be eradicated in $\sum_{n=1}^i n k_n + \tau$ days.

Proof. According to the second phase of the proposed model, if both $X_I(t)$ and $X_{Q_I}(t)$ are non-negative functions concerning t , then $\frac{dY}{dt} \geq 0$, which implies $Y(t)$ is an increasing function.

Then, following the theorem conditions, for each m ($1 \leq m \leq \tau$), we have $Y(T_{i,k_i} + m) = Y(T_{i,k_i})$. Thus, $X(t) = X_I(t) = X_{Q_I}(t) = 0$ for $T_{i,k_i} \leq t \leq T_{i,k_i} + \tau$, we further have $f_S(t) = f_E(t) = f_I(t) = 0$.

According to the definition of $f_S(t)$, $f_E(t)$ and $f_I(t)$, we have $E(t) = 0$, $I(t) = 0$.

In this study, regardless how large the value R_0 and what the vaccination rate are, and whether the virus mutates, the solution (S, E, I, R) would be convergent to the disease-free equilibrium (DFE) if the conditions of the theorem are satisfied. This means that the epidemic will be effectively eradicated under the ‘‘Dynamic Zero-COVID’’ policy.

3.2. Transmission risk and prevention and control capability indexes

In the process of the epidemic prevention and control, the implementation of intervention measures are not static. The local epidemiological situation determines the adjustment of prevention and control measures. Reviewing the Yangzhou epidemic, the testing time interval has been adjusted many times and the testing area has also changed from the whole to the part. The epidemiological situation is closely related to the prevention and control capacity of the public health system. To better understand and illustrate the mechanism of Yangzhou’s successful prevention and control mechanism, we first define the basic reproductive number as an important epidemiological index based on the proposed models, to quantify the risk level of disease transmission, and then design the index of public health prevention and control ability describing the ability of relevant departments to deal with the epidemic risk.

3.2.1. Basic and effective reproductive numbers

The basic reproductive number is a widely used quantitative indicator to evaluate the transmission potential. Depending on the proposed models (I) and (II), we have the expressions of the basic reproductive number, R_0 , before and after intervention at the disease-free equilibrium with the next-generation matrix method for the compartment system without [30] and with time delays [31], describing the average number of secondarily infected individuals by being directly infected by a single infectious individual in a completely susceptible population without and with interventions during its infectious period,

$$R_0 = \begin{cases} \frac{\beta c_1}{r_1}, & \text{without interventions,} \\ \frac{\beta c_2}{r_1 + \theta(i) \frac{1}{k_i}}, & \text{with interventions,} \end{cases}$$

where $\theta(i)$ denotes the accuracy rate of repeated i testing. See Models 2.1 part for specific expressions.

R_0 is independent of the total population. By comparing the R_0 before the intervention, three factors, namely repeated testing rounds (i), the duration for i -round testing (k_i), and daily number of primary contacts per case (c_1, c_2), affect the R_0 value after the intervention. If $R_0 < 1$, the epidemic will persist, and if $R_0 > 1$, the epidemic will reverse. We can have $R_0 < 1$ equivalent to

the following expression:

$$k_i < \frac{\theta(i)}{\beta c_2 - r_1}, \text{ when } \beta c_2 > r_1.$$

This means that the time interval between the $i + 1$ -round and i -round testing should be less than a specific value if the epidemic is effectively suppressed.

We also introduce a time-dependent transmission risk index, the effective number $R_e(t)$, to quantify the total number of people infected by one case at time t when the target population is not all susceptible [32],

$$R_e(t) = \begin{cases} \frac{\beta c_1}{r_1} \cdot \frac{S(t)}{N_0}, & t < T_1, \\ \frac{\beta c_2}{r_1 + \theta(i) \frac{1}{k_i}} \cdot \frac{S(t)}{N_0 - Q(t)}, & t \geq T_1. \end{cases}$$

3.2.2. Public health prevention and control force

The public health department has paid more attention to tackling the risks posed by the spread of the disease; its intuitive performance is to find the infected and isolate the contacts as soon as possible through the TTI strategy. This means that the prevention and control force of public health at time t is closely associated with the size of the confirmed cases and the isolated people. Based on our models and epidemic data, to better quantify public health prevention and control efforts, we will offer the mathematical expression of public health prevention and control force in response to the change in disease transmission risk. Here, we define a time-varying public health prevention and control force index marked by $CF(t)$, which depends on the ratio of cumulative diagnosed to cumulative infected cases denoted by $P_I(t)$ and the ratio of cumulative isolated persons to cumulative close contacts denoted by $P_Q(t)$. The larger the values of $P_I(t)$ and $P_Q(t)$, the stronger the public health prevention and control force will be. $CF(t)$ needs to satisfy the following:

- i. $CF(P_I(t), P_Q(t))$ is continuous differentiable for $P_I(t) \in [0,1]$ and $P_Q(t) \in [0,1]$ for any t ,
- ii. $\lim_{(P_I, P_Q) \rightarrow (0,0)} CF(0,0) = 0$, $\lim_{(P_I, P_Q) \rightarrow (1,1)} CF(1,1) = 1$,
- iii. $CF(P_I, 0) \neq 0, CF(0, P_Q) \neq 0$,
- iv. $\frac{dCF}{dP_I} > 0$ and $\frac{dCF}{dP_Q} > 0$ for any $P_I \in (0,1)$ and $P_Q \in (0,1)$,

For simplicity, in this study we take

$$CF(t) = \frac{1}{1-e^{-1}} e^{-(1-P_I(t))(1-P_Q(t))} - \frac{e^{-1}}{1-e^{-1}},$$

with

$$P_I(t) = \frac{\text{Cumulative confirmed cases at time } t}{\text{Cumulative infected cases at time } t}$$

$$= \begin{cases} 0, & t < T_1, \\ \frac{\sum_{s=T_1}^t X(s)}{\sum_{s=T_0}^{T_1} \beta c_1 \frac{I(s)}{N(s)} S(s) + \sum_{s=T_1}^t \beta c_2 \frac{I(s)}{N(s)} S(s)}, & t \geq T_1, \end{cases}$$

and

$$P_Q(t) = \frac{\text{Cumulative isolated contacts at time } t}{\text{Cumulative primary and second contacts at time } t}$$

$$= \begin{cases} 0, & t < T_1, \\ \frac{\sum_{s=T_1}^t (f_S(s) + f_E(s) + f_I(s))}{\sum_{s=T_1}^t (1 + c_s) c_2 X(s)}, & t \geq T_1, \end{cases}$$

where $X(s)$ is the daily total number of newly confirmed cases on day t , and f_S , f_E and f_I are the total numbers of susceptible, latent and infectious individuals into Q due to Testing-Tracing-Isolation (TTI) policy on day t , respectively. All of their expressions, including specific expressions, are seen in Subsection 2.2.

4. Numerical results

To more intuitively explain the mechanism of the “Dynamic Zero COVID-19” strategy implemented for Yangzhou’s epidemic, we will first fit the collected data with the models to estimate some uncertain parameter values shown in Table 1. Then, we will explore the correlation of some parameters, including duration of free transmission phase, testing population scale, the time interval of each round of testing, isolation duration, etc., with the cumulative confirmed cases and isolated people by sensitivity analysis. Furthermore, we will simulate the changes in the daily confirmed cases, the isolated population size and the maximum testing times required for successful “Dynamic Zero COVID-19” under different scenarios.

4.1. Parameter estimation

Applying the proposed model with some parameters fixed at default values in Table 1, we fit the daily confirmed cases in/outside IZs, daily total confirmed cases and cumulative isolated contacts in the epidemic area of Yangzhou, China, from July 21 to Aug. 31, 2021, to calibrate five uncertain parameters in Table 1 and the final size of isolated people. We performed the parameter fitting by using an adaptive Metropolis-Hasting algorithm carrying out the Markov Chain Monte Carlo (MCMC) procedure with 50,000 iterations and a burn-in of the first 20,000 iterations in MATLAB R2019b [33]. We estimated the final size of isolated people for Yangzhou’s epidemic to be about 19,870 (95%CI 13,070, 26,840). The relevant results are displayed in Figure 4. The estimated parameter values and their confidence intervals are listed in Table 1.

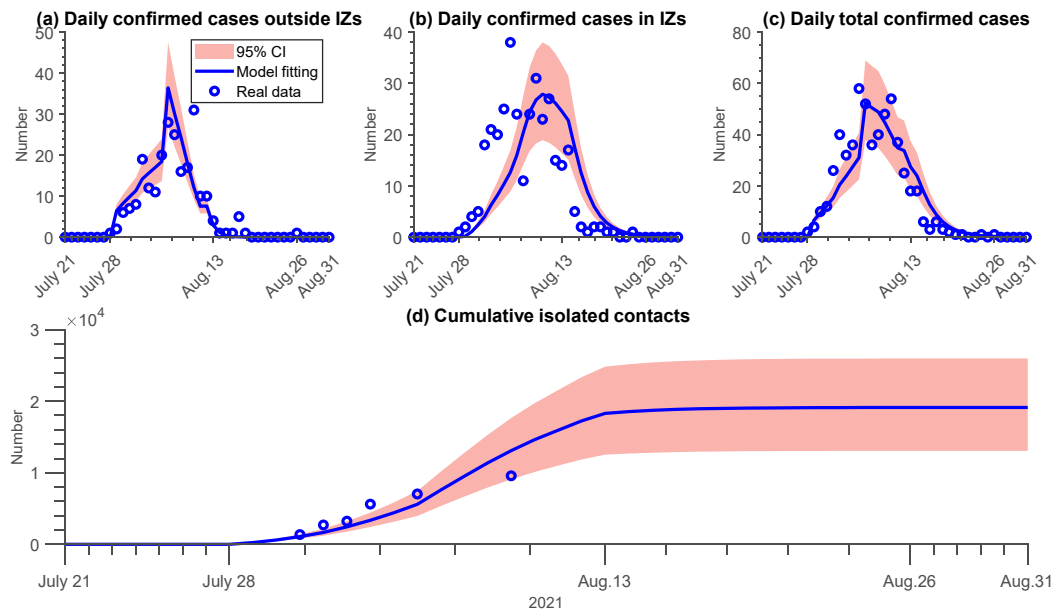


Figure 4. Model fitting for the daily confirmed cases in/outside IZs, daily total confirmed cases and cumulative isolated contacts in Yangzhou from July 21 to Aug. 31, 2021. The circles represent reported data, the solid lines are the fitting results and the light-shaded area shows the 95% confidence interval (CI). Data resources form [24] and [25].

4.2. Simulations

4.2.1. Transmission risk and public health prevention and control force

To better reveal the successful mechanism of fighting COVID-19 in Yangzhou, we quantified the effective reproductive number and the prevention and control force over time. As can be shown in Figure 5, the overall risk of the epidemic transmission decreased over time, while the prevention and control effort increased. Before KTTI, the transmission risk had already been at a relatively low level ($R_e = 1.14$) and the public health department had made great efforts ($CF = 0.97$).

The epidemic in Yangzhou eventually infected 572 people and quarantined nearly 19,870 people.

For the main urban area of Yangzhou with a population of 1.7 million, the change of $\frac{S(t)}{N_0 - Q(t)}$ over time was estimated to be relatively small during the whole epidemic process, so the effective reproductive number (R_e) is mainly determined by the basic reproductive number (R_0). We estimated the basic reproductive number without interventions as $R_0 = 6.98$. In the process of combating Yangzhou's epidemic, the testing interval was continuously adjusted from 4 days to 1 day; it took about six rounds of CTTI before the transmission risk dropped to nearly 1. Once the testing interval was greater than 1, the transmission risk would rebound, unless it began to implement KTTI accurately once a day and further limited contact between people in the community. It can be seen that the testing interval played a vital role in the elimination of Yangzhou's epidemic. According to the equivalent formula of $R_0 < 1$, if the accuracy of each test can be maintained at 0.8, the interval between two rounds of CTTI should be less than 1.4 days to make the risk of the epidemic transmission less than 1

as soon as possible. Combined with the definition of R_0 , the findings highlight the challenges of implementing the “Dynamic Zero COVID-19” strategy and the need for joint efforts of relevant departments and citizens.

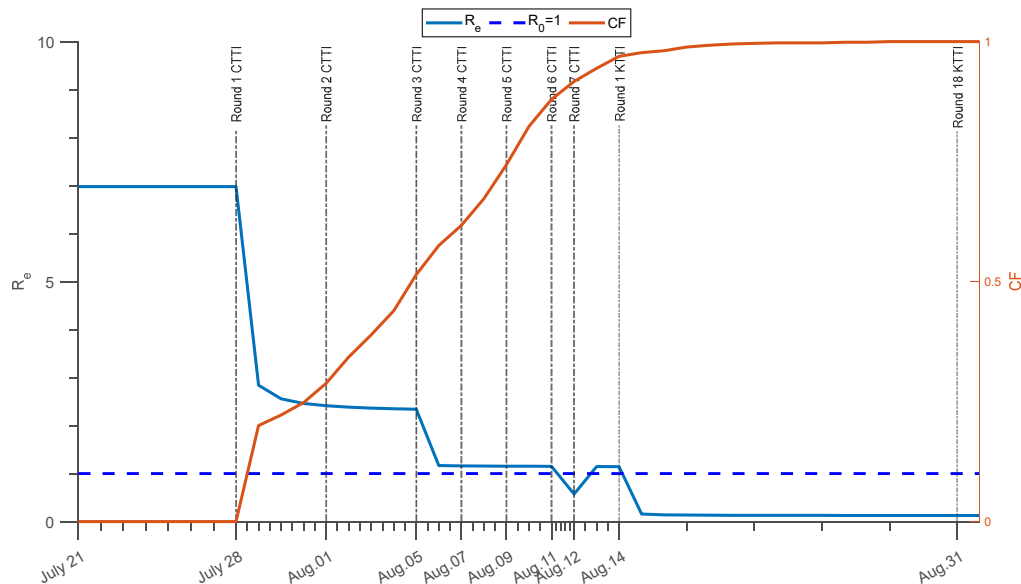


Figure 5. The changes in transmission risk and prevention and control force indicators over time in the process of the epidemic prevention and control in Yangzhou: the effective reproductive number (blue solid line with the vertical axis on the left), transmission risk threshold value (blue dash line) and the prevention and control force (red solid line with the vertical axis on the right). Thick and thin black dash lines represent city-wide testing and key area testing respectively. CTTI: city-wide test-trace-isolation, KTTI: key area test-trace-isolation.

4.2.2. Impact of prevention and control modes

Figure 6 compares the daily number of newly confirmed or infected cases over time under three scenarios: testing only without tracing, Yangzhou’s zero COVID-19 and no intervention. For Yangzhou’s epidemic, it was finally brought under control in 42 days (on Aug. 31) after no case was reported for five consecutive days. The total number of confirmed cases stood at 572, with the daily new confirmed cases reaching 58 on Aug. 05. Numerical results indicate that if only testing is carried out without tracing, the end of the outbreak will be delayed by four days and the final size of infections will reach 1,417, peaking at 155 on Aug. 12, which are respectively increased by 148 and 167% as those of Yangzhou’s situation. If no control measures are taken, the outbreak will be so severe that the vast majority of people may be infected; without the impact of a vaccine, the epidemic could not be controlled until Dec. 04.

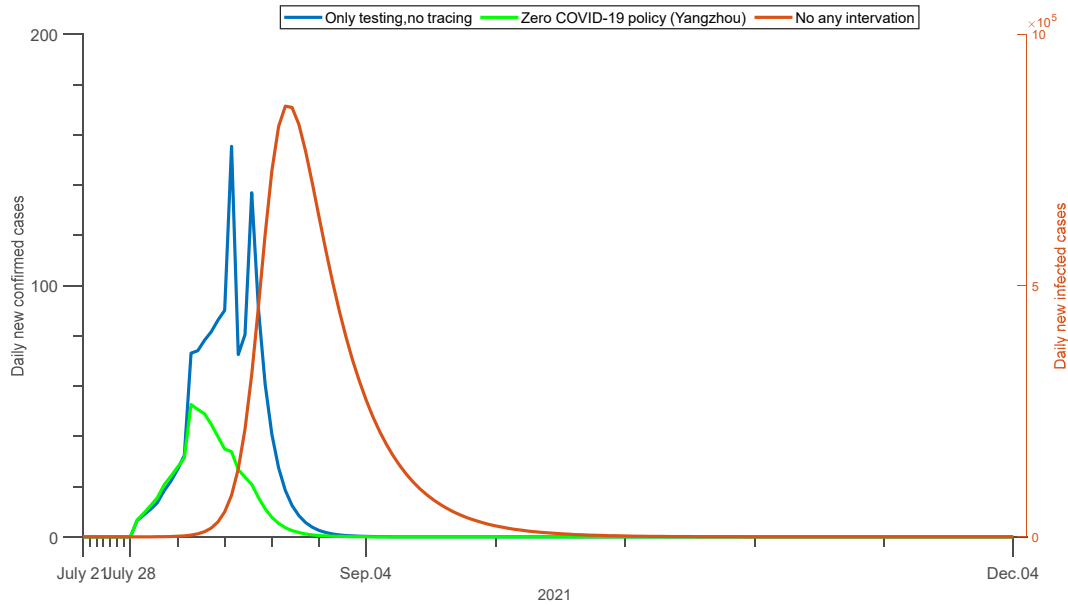


Figure 6. The effect of different prevention and control modes on daily new confirmed (infected) cases over time: only testing without tracing (blue line with the vertical axis on the left), Yangzhou’s epidemic (green line with the vertical axis on the left) and no any intervention (red line with the vertical axis on the right).

4.2.3. Impact of duration of the free transmission phase

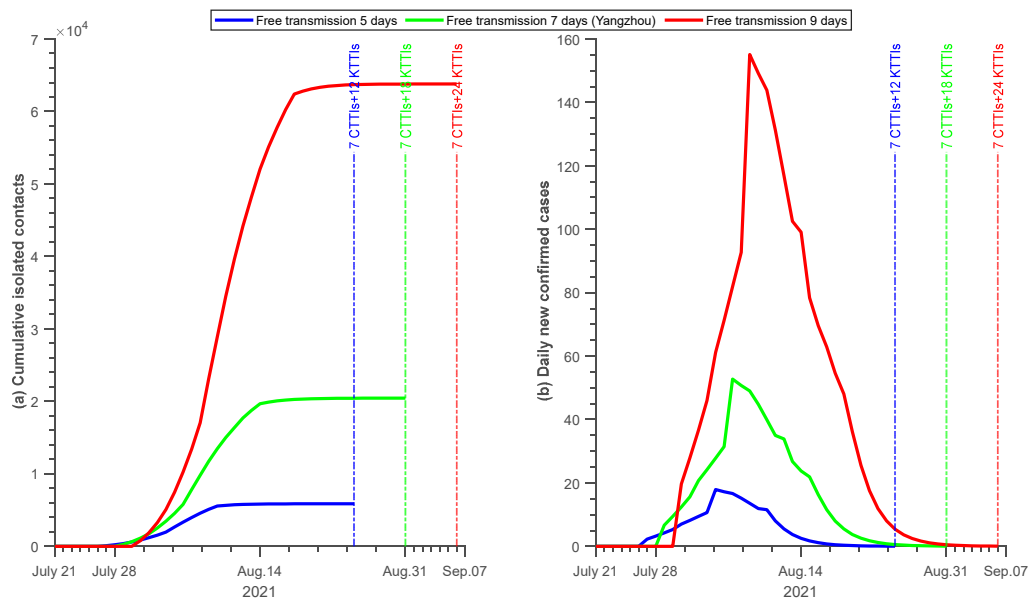


Figure 7. The effect of the duration of the free transmission phase on the cumulative isolated contacts (a) and the daily new confirmed cases (b) with the minimum testing rounds under three durations: 5 days (green), 7 days (blue) and 9 days (red). CTTI: city-wide test-trace-isolation, KTTI: key area test-trace-isolation.

Figure 7 shows the impact of different durations of free transmission phases on the epidemic prevention and control in Yangzhou. Compared with the 7-day free transmission phase in the Yangzhou epidemic, if the duration is reduced by two days, the outbreak will be curbed in 36 days (Aug. 25) after 7 rounds of CTTIs and 12 rounds of KTTIs, where the total numbers of infected and isolated people (180 and 5,938) will be down by 68.5 and 73.0%, respectively, and the peak time with a peak value of 18 will be 1 day earlier. If the duration is delayed for two days, it will take 7 rounds of CTTIs and 24 rounds of KTTIs and 48 days (Sep. 06) to achieve zero COVID-19, and the final sizes of infections and isolations (17,694 and 64,126) will be increased by 209.3 and 222.7%, respectively, and the peak time with a peak of 156 would be 2 days later.

4.2.4. Impact of tracking efficiency

For the Yangzhou outbreak, we estimated that the isolated contacts accounted for only 55% of the actual contacts, which implied that nearly half of the primary and secondary contacts may not be tracked. To further explore the impact of different tracking rates on the containment of the epidemic, we plot the development of cumulative isolated contacts and the daily new confirmed cases over time when the tracking rate is increased and decreased by 20%, as shown in Figure 8. If the tracking rate is reduced by 20%, the epidemic in Yangzhou will end on Aug. 30 with a total of 676 infections and 16,600 isolated contacts after 7 rounds of CTTIs and 17 rounds of KTTIs. If the tracking rate is increased by 20%, the outbreak will be brought under control on Sep. 02 after 7 rounds of CTTIs and 20 rounds of KTTIs, the total infected and isolated people stand at 563 and 24,360, respectively. Compared with the peak value in Yangzhou, the decrease (increase) of the tracking rate will increase (decrease) the peak value from 58 to 60 (46) but has little influence on the peak time. The results show that although the increase in tracking rate can add to the total isolated population to some extent, the final size of infections eventually goes down.

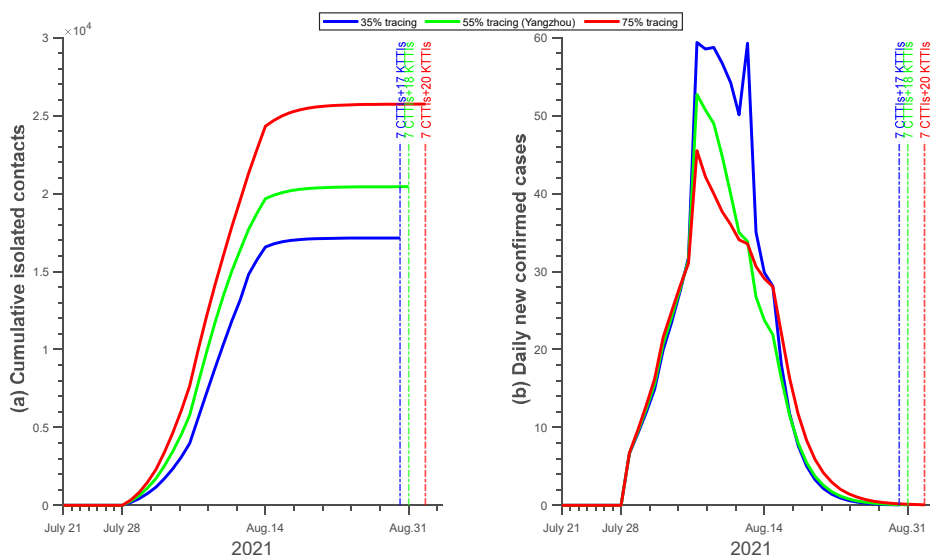


Figure 8. The effect of tracking efficiency on the cumulative isolated contacts (a) and the daily new confirmed cases (b) with the minimum testing rounds under three scenarios: 35% tracking (green), 55% tracking (blue) and 75% tracking (red).

4.2.5. Impact of a mean time interval of testing

Based on the definitions of basic (effective) reproductive number, the impact of testing interval on the epidemic transmission risk is a critical parameter. Therefore, we examined the impacts of different intervals on the total number of isolations and infections, peak value, peak arrival time, epidemic duration, and the minimum number of detection rounds. Since the basis for the transformation from CTTI to KTTI has not been clarified, we also simulated implementing CTTI 7 times before KTTI to ensure KTTI is only put into operation when the transmission risk is low. Figure 9 shows the cumulative isolated contacts and the daily new confirmed cases with the minimum testing rounds for different interval between two tests: 1 day/round, 3 days/round, 4 days/round and 5 days/round. We found that when the interval is 1, 3, 4 or 5 days, the peak time of the epidemic will arrive from 9, 18, 29 to 44 days with increased peak values of 21, 27, 62 and 602 infected, respectively. Besides 7 rounds of CTTIs, 16, 6, 7 and 17 rounds of KTTIs will be needed for the corresponding intervals before the epidemic ends. Additionally, the epidemic final size increases from 120, 421, 1,382 to 12,049, the epidemic lasts for 31, 46, 61 and 126 days, and the isolated increases from 3,989, 15,590, 48,904 to 302,860, respectively, see Table 2 for details. One can see that the longer the average interval is, the more severe the outbreak will be. However, the minimum testing round is not positively correlated with the average interval. This result illustrates that the epidemic is effectively controlled in a short time, a large amount of investment in medical resources is indispensable.

4.2.6. Impact of the precise division of key areas

As the policy was mandated, most citizens were able to live and work except for some enclosed areas when CTTI was started. However, when implementing KTTI, the personnel in key areas are required to stay at home. The number of close contacts was reduced by the adjustment of CTTI to KTTI, which is consistent with our estimation that two parameters about the number of primary and second contacts (c_2, c_s) have changed. Next, we analyzed the impacts of the implementation of CTTI and KTTI at the beginning of the outbreak on the daily new infections and cumulative isolations, see Figure 10. Compared with Yangzhou's outbreak, we found that KTTI has been implemented all the time, and the epidemic will achieve excellent results. The epidemic will end 10 days in advance after only 15 rounds of KTTIs (on Aug. 21), of which the total numbers of infections and isolations are 106 and 898, respectively. The implementation of CTTI has significantly reduced the effect of epidemic prevention and control. The epidemic will be delayed for 40 days (on Oct. 06). The minimum round number of CTTIs is up to 55, leading to 682 infections and 26,560 isolations. Therefore, it can be seen that accurately locating key areas and implementing KTTI is very important for the epidemic prevention and control, which can not only quickly curb the epidemic in a short time, but also save a lot of resources.

Table 2. Prevalence values under different testing intervals.

Testing interval (day/round)	Total isolations	Total infections	Peak arrival time (days)	Peak value	Total rounds (CTTI+KT TI)	Epidemic duration (days)
1	3,989	120	9	21	7+16	31
3	15,590	421	18	27	7+6	46
Yangzhou	19,870	572	16	58	7+18	42
4	48,904	1,382	29	62	7+7	61
5	302,860	12,049	44	602	7+17	126

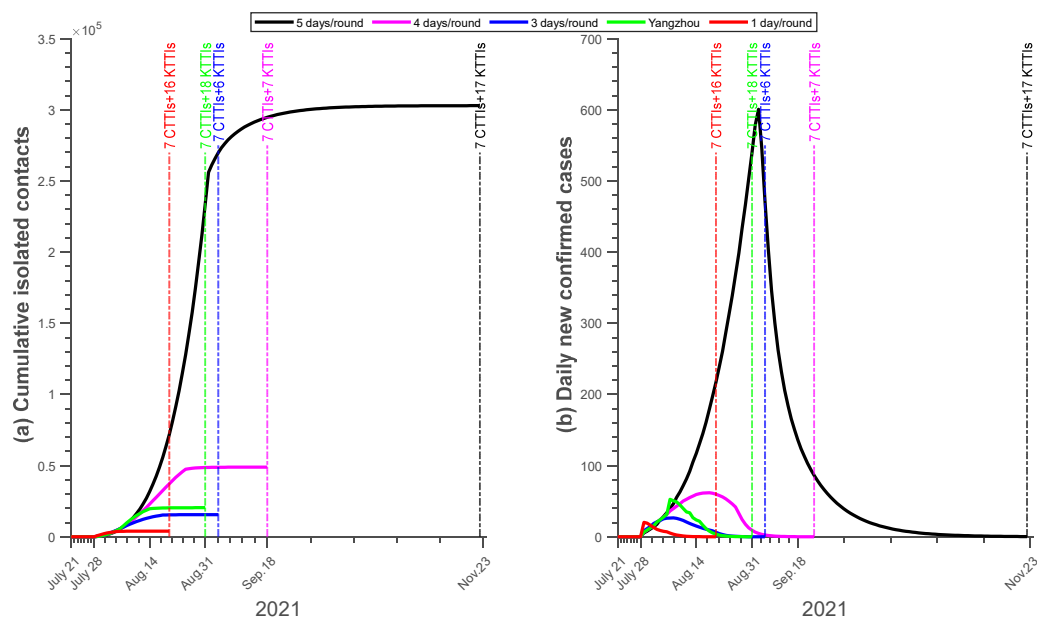


Figure 9. The effect of testing interval on the cumulative isolated contacts (a) and the daily new confirmed cases (b) with the minimum testing rounds under five scenarios: 1 day/round (red), 3 days/round (blue), Yangzhou's situation (green), 4 days/round (purple) and 5 days/round (black).

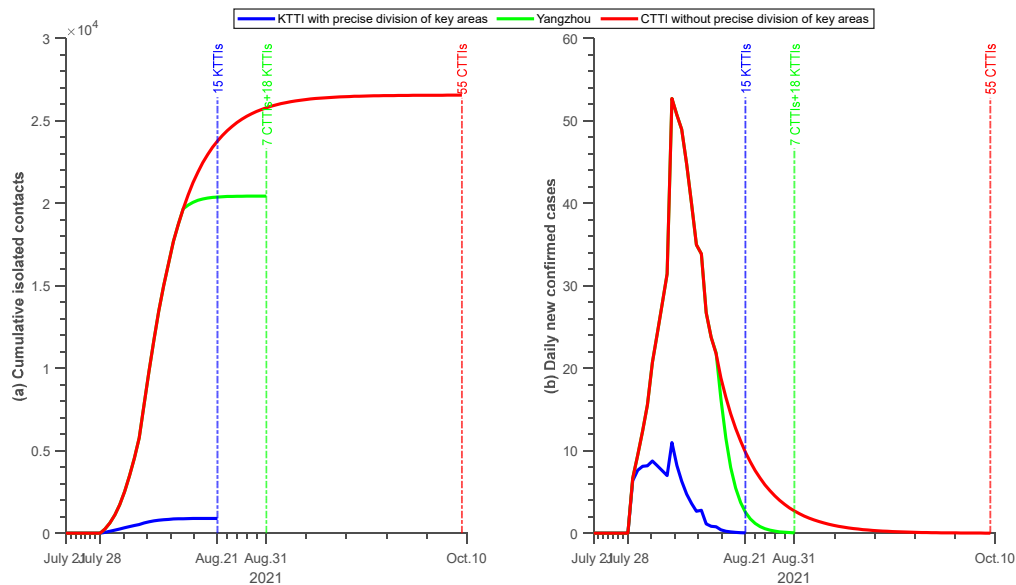


Figure 10. The effect of the accurate division of key areas on the cumulative isolated contacts (a) and the daily new confirmed cases (b) with the minimum testing rounds under three scenarios: KTTI with precise division of Key areas (blue), Yangzhou’s situation (green), CTTI without precise division of Key areas (red).

4.3. Sensitivity analysis

We are interested in examining the sensitivity of the total confirmed cases and isolated people on some zero policy-related parameters, including tracing efficiency (δ), duration of free transmission phase ($T_1 - T_0$), the time interval between two tests (k), primary contact number per case (c_1) and the testing accuracy rate (θ). We employed the well-known Latin Hypercube Sampling/Partial Rank Correlation Coefficient (LHS/PRCC) method [34] by generating 2,000 samples and varying the corresponding parameter values of their given values (see Table 1). We verified the relationship between those parameters and the outcomes, evaluated the PRCC values and plotted Figure 11.

From Figure 11, the final sizes of infected cases and isolated people had a significant correlation with the above five parameters ($p < 0.05$), which reflects the challenge of all links in the implementation of the “Dynamic zero COVID-19” policy. Total confirmed cases and isolated people present a positive correlation with duration of free transmission, time interval between two testing and primary contact number per case, but a negative correlation with testing accuracy rate. However, tracing efficiency is negatively associated with the final size of infected cases but positively associated with that of isolated people. Sensitivity analysis also illustrates that the fight against the epidemic is not only necessary to find the source of infection as soon as possible (i.e., quickly carry out testing and improve the efficiency of testing and tracking), but also for the public to protect themselves and abide by relevant policies and regulations.

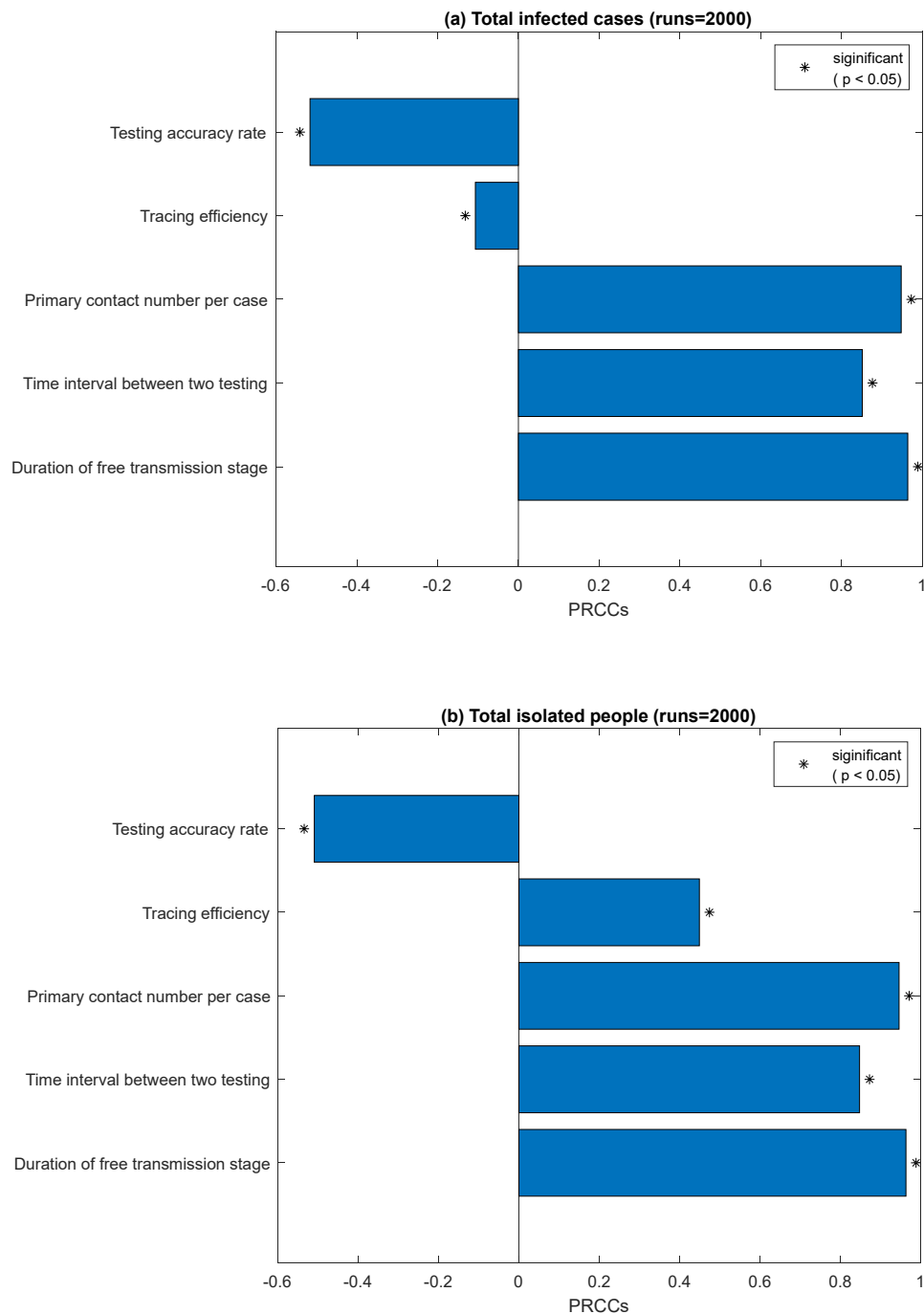


Figure 11. PRCC plots of different parameters on the final sizes of infected cases (a) and isolated people (b).

5. Discussion and conclusions

Facing the unprecedented crisis brought by the unexpected COVID-19, the “Dynamic Zero COVID-19” strategy was adopted to control the local epidemic. This study took the Yangzhou outbreak as a case study and constructed a dynamic model with multiple rounds of CTTIs and KTTIs. Based on the proposed model, we defined two time-varying indicators to describe the risk of disease

transmission and the prevention and control force of public health in the process of the “Dynamic Zero COVID-19” strategy implemented in Yangzhou. Along with the available data and literature parameters, we simulated and analyzed the occurrence and development of Yangzhou’s epidemic. This study adopts a more intuitive empirical analysis method, making people deeply understand the concept of elimination strategy and its role in controlling the epidemic. At the same time, some research results also provide theoretical support for adjusting relevant policies.

Speed is one of the cores of the “Dynamic Zero COVID-19” strategy, which has been fully reflected in dealing with the epidemic in Yangzhou. Our findings suggest that multiple rounds of testing-trace-isolation play a crucial role in effectively achieving the epidemic prevention goal, especially with rapid testing. During the Yangzhou epidemic, the longer the average testing interval was, the more serious the epidemic would be. The testing interval has been continuously adjusted from 4 days/round to 1 day/round. After six rounds of CTTIs, the epidemic transmission risk was less than 1. According to the actual situation in Yangzhou, under the condition of ensuring the detection accuracy of 80%, we estimated that the average detection interval should be less than 1.4 days/round to reduce the risk of the epidemic transmission effectively. This result provides theoretical support for the determination of the testing time in the notice issued by the National Health Protection Commission of China on March 22, 2022, which is the implementation of the nucleic acid testing organization (Third Edition). The policy explicitly requires that all districts and cities, regardless of the population size, match the sampling and detection force according to the goal of completing the city’s nucleic acid detection within 24 hours [35].

According to the quantitative analysis of Yangzhou’s outbreak, we found that there is not necessarily a positive correlation between the minimum number of test rounds and the testing speed. From the perspective of the effect of the epidemic prevention and control, one test per day is the best, which can limit the epidemic infection at the minimum scale in a short time. However, the minimum testing number even exceeds that of 3 days/round. This means that many resources must be invested to be effectively curbed in a short time. In order to achieve the maximum prevention and control effect at the least cost and minimize the impact of the epidemic on economic and social development, further studies with comprehensive economic assessment may bring us some enlightenment and deep thoughts.

The Delta virus that caused the epidemic in Yangzhou spread quite quickly. Its basic reproductive number was estimated to be 6.98, surpassing the previous strains. Once the duration of the free transmission phase is extended, the final size of the infections will significantly increase, even by as much as 200% with the 2-day delay (Figure 7). Our research results show that improving the efficiency of all links of prevention and control plays an active role in reducing the spread of the epidemic diseases and protecting people’s health. The first is to improve the monitoring efficiency, detect the epidemic situation in time, and reduce the time of free transmission stage (Figure 7). Second, one should improve the efficiency of tracking and isolation. For infected persons, through epidemiological investigation, one must identify and isolate their primary and secondary contacts as soon as possible. Although tracking and isolation increase the quarantined personnel to a certain extent, it will reduce the number of final infections (Figure 8). Third, one should improve the efficiency of public self-protection and reduce human contact (Figure 11).

Notably, in the face of a sudden outbreak, how to decide whether to implement CTTI or KTTI? If CTTI is implemented in advance, when and under what conditions can it be adjusted to KTTI? The corresponding quantitative analysis is not given in our study, which is also worthy of further research in the future. During the implementation of the “Dynamic Zero COVID-19” policy by Yangzhou, our

results show that KTTIs began after 6 rounds of CTTIs with a low risk of disease transmission. With the presupposition that all infectious people outside IZ should be on the list of testing in each round of KTTI, we found that the size of the test population did not affect the speed of diagnosis of infected people at a given detection interval. Therefore, precisions should be another core of the “Dynamic Zero COVID-19” strategy, and will be a prerequisite for answering the above concerns. If we can accurately locate the epidemic prevention and control area through epidemiological investigation, it will be a decisive factor to reduce the cost of the epidemic prevention and control and minimize the impact of the epidemic on social development.

China’s “Dynamic Zero COVID-19” strategy does have its unique advantages. Our theoretical analysis shows that a strict “Dynamic Zero COVID-19” strategy can effectively eliminate local transmission regardless of the risk of disease transmission, virus mutation, and vaccine coverage. However, the implementation of this strategy is a challenging project. The implementation of rapid and precise prevention and control requires not only sufficient human resources, financial and material resources, but also the coordination and cooperation of multiple departments, as well as the active collaboration of the general public; this limits its applicability in other regions. Although some countries have tried to liberalize, the epidemic prevention policies of various countries and regions have not been completely abolished, and they are constantly adjusted to mitigate the impact of the epidemic. Adequate policies depend not only on people’s social preferences and government capacity, but also on an accurate understanding of the costs and benefits of different COVID-19 responses [36]. Despite the many adverse effects of the outbreak, with increasing awareness and research on COVID-19, effective progress has been made in controlling the spread of the disease and reducing the fatality rate through vaccination and public health measures. Therefore, both countries and individuals should be full of confidence in victory, and optimistic in the face of the outbreak.

Use of AI tools declaration

The authors declare they have not used Artificial Intelligence (AI) tools in the creation of this article.

Acknowledgments

This work was financially supported by National Natural Science Foundation of China (No. 12201562), Chongqing Support Program for Returning Overseas Scholars (No. cx2022077) and One Health Modelling Network for Emerging Infections (OMNI) of the Natural Sciences and Engineering Research Council of Canada.

Conflict of interest

The authors declare there is no conflict of interest.

References

1. CSSE: COVID-19 Dashboard, Johns Hopkins University (JHU), 2022. Available from: <https://www.arcgis.com/apps/dashboards/bda7594740fd40299423467b48e9ecf6>.

2. WHO: Tracking SARS-CoV-2 variants, 2022. Available from: <https://www.who.int/en/activities/tracking-SARS-CoV-2-variants/>.
3. T. K. Burki, Omicron variant and booster COVID-19 vaccines, *Lancet Respir. Med.*, **10** (2022). [https://doi.org/10.1016/S2213-2600\(21\)00559-2](https://doi.org/10.1016/S2213-2600(21)00559-2)
4. Y. Liu, J. Rocklöv, The reproductive number of the Delta variant of SARS-CoV-2 is far higher compared to the ancestral SARS-CoV-2 virus, *J. Travel Med.*, **28** (2021), 1–3. <https://doi.org/10.1093/jtm/taab124>
5. MMWR: Centers for Disease Control and Prevention, 2022. Available from: <https://www.cdc.gov/mmwr/volumes/71/wr/mm7104e4.htm>.
6. O. Barnes, J. Burn-Murdoch, Omicron’s less severe cases prompt cautious optimism in South Africa, 2021. Available from: <https://www.ft.com/content/d315be08-cda0-462b-85ec-811290ad488e>.
7. WHO: WHO Director-General’s opening remarks at the media briefing – 5 May 2023, 2023. Available from: <https://www.who.int/director-general/speeches/detail/who-director-general-s-opening-remarks-at-the-media-briefing---5-may-2023>.
8. M. Oliu-Barton, B. S. R. Pradelski, Y. Algan, M. G. Baker, A. Binagwaho, G. J. Dore, et al., Elimination versus mitigation of SARS-CoV-2 in the presence of effective vaccines, *Lancet Global Health*, **10** (2022), e142–e147, 2022. [https://doi.org/10.1016/S2214-109X\(21\)00494-0](https://doi.org/10.1016/S2214-109X(21)00494-0)
9. M. Oliu-Barton, B. S. R. Pradelski, P. Aghion, P. Artus, I. Kickbusch, J. V. Lazarus, et al., SARS-CoV-2 elimination, not mitigation, creates best outcomes for health, the economy, and civil liberties, *Lancet*, **397** (2021), 12–18. [https://doi.org/10.1016/S0140-6736\(21\)00978-8](https://doi.org/10.1016/S0140-6736(21)00978-8)
10. W. Liang, M. Liu, J. Liu, Y. Wang, J. Wu, X. Liu, The dynamic COVID-zero strategy on prevention and control of COVID-19 in China (in Chinese), *Chin. Med. J.*, **102** (2022), 239–242. <https://doi.org/10.3760/cma.j.cn112137-20211205-02710>
11. Coexist with COVID-19’ for only ten days, the number of critically ill cases in Korea has reached a new high (in Chinese), 2021. Available from: <https://baijiahao.baidu.com/s?id=1716037339938236108&wfr=spider&for=pc>.
12. Y. Xing, G. Wong, W. Ni, X. Hu, Q. Xing, Rapid response to an outbreak in Qingdao, China, *N. Engl. J. Med.*, **383** (2020), e129. <https://doi.org/10.1056/nejmc2032361>
13. Z. Wu, Q. Wang, J. Zhao, P. Yang, J. M. McGoogan, Z. Feng, et al., Time course of a second outbreak of COVID-19 in Beijing, China, June–July 2020, *JAMA*, **324** (2020), 1458–1459. <https://doi.org/10.1001/jama.2020.15894>
14. Z. Li, F. Liu, J. Cui, Z. Peng, Z. Chang, S. Lai, et al., Comprehensive large-scale nucleic acid–testing strategies support China’s sustained containment of COVID-19, *Nat. Med.*, **27** (2021), 740–742. <https://doi.org/10.1038/s41591-021-01308-7>
15. *New Coronavirus Pneumonia Diagnosis and Treatment Plan (Trial Version 8) (in Chinese)*, National Health Commission of the People’s Republic of China, 2020. Available from: <http://www.nhc.gov.cn/yzygj/s7653p/202008/0a7bdf12bd4b46e5bd28ca7f9a7f5e5a.shtml>.
16. Y. Zhang, C. You, X. Gai, X. Zhou, On coexistence with COVID-19: estimations and perspectives, *China CDC Wkly*, **3** (2021), 1057–1061. <https://doi.org/10.46234/ccdcw2021.245>
17. B. Tang, F. Xia, S. Tang, N. L. Bragazzi, Q. Li, X. Sun, et al., The effectiveness of quarantine and isolation determine the trend of the COVID-19 epidemic in the final phase of the current outbreak in China, *Int. J. Infect. Dis.*, **95** (2020), 288–293. <https://doi.org/10.1016/j.ijid.2020.03.018>

18. C. Hou, J. Chen, Y. Zhou, L. Hua, J. Yuan, S. He, et al., The effectiveness of quarantine of Wuhan city against the Corona Virus Disease 2019 (COVID-19): a well-mixed SEIR model analysis, *J. Med. Virol.*, **92** (2020), 841–848. <https://doi.org/10.1002/jmv.25827>
19. K. Shimizu, T. Kuniya, Y. Tokuda, Modeling population-wide testing of SARS-CoV-2 for containing COVID-19 pandemic in Okinawa, Japan, *J. Gen. Fam. Med.*, **22** (2021), 173–181. <https://doi.org/10.1002/jgf2.439>
20. A. Aleta, D. Martín-Corral, A. P. Y. Piontti, M. Ajelli, M. Litvinova, M. Chinazzi, et al., Modelling the impact of testing, contact tracing and household quarantine on second waves of COVID-19, *Nat. Hum. Behav.*, **4** (2020), 964–971. <https://doi.org/10.1038/s41562-020-0931-9>
21. T. Colbourn, W. Waites, J. Panovska-Griffiths, D. Manheim, S. Sturniolo, G. Colbourn, et al., Modelling the health and economic impacts of population-wide testing, contact tracing and isolation (PTTI) strategies for COVID-19 in the UK, *SSRN Electron. J.*, **9** (2020). <https://doi.org/10.2139/ssrn.3627273>
22. A. J. Kucharski, P. Klepac, A. J. K. Conlan, S. M. Kissler, M. L. Tang, H. Fry, et al., Effectiveness of isolation, testing, contact tracing, and physical distancing on reducing transmission of SARS-CoV-2 in different settings: a mathematical modelling study, *Lancet Infect. Dis.*, **20** (2020), 1151–1160. [https://doi.org/10.1016/s1473-3099\(20\)30457-6](https://doi.org/10.1016/s1473-3099(20)30457-6)
23. S. Contreras, J. Dehning, M. Loidolt, J. Zierenberg, F. P. Spitzner, J. H. Urrea-Quintero, et al., The challenges of containing SARS-CoV-2 via test-trace-and-isolate, *Nat. Commun.*, **12** (2021), 378. <https://doi.org/10.1038/s41467-020-20699-8>
24. Yangzhou city health and family planning commission website, 2021. Available from: <http://wjw.yangzhou.gov.cn/>.
25. The paper news official website, 2021. Available from: <https://www.thepaper.cn/>.
26. A. Holborow, H. Asad, L. Porter, P. Tidswell, C. Johnston, I. Blyth, et al., The clinical sensitivity of a single SARS-CoV-2 upper respiratory tract RT-PCR test for diagnosing COVID-19 using convalescent antibody as a comparator, *Clin. Med.*, **20** (2020), 6. <https://doi.org/10.7861/clinmed.2020-0555>
27. J. Chhatwal, Y. Xiao, P. Mueller, M. Adee, O. O. Dalgic, M. A. Ladd, et al., Changing dynamics of COVID-19 in the U.S. with the emergence of the Delta variant: projections of the COVID-19 simulator, *medRxiv*, 2021. <https://doi.org/10.1101/2021.08.11.21261845>
28. B. Li, A. Deng, K. Li, Y. Hu, Z. Li, Y. Shi, et al., Viral infection and transmission in a large well-traced outbreak caused by the Delta SARS-CoV-2 variant, *Nat. Commun.*, **13** (2022). <https://doi.org/10.1038/s41467-022-28089-y>
29. M. Du, M. Liu, J. Liu, Progress in research of epidemiologic feature and control of SARS-CoV-2 Delta variant (in Chinese), *Chin. J. Epidemiol.*, **42** (2021), 1774–1779. <https://doi.org/10.3760/cma.j.cn112338-20210808-00619>
30. P. Dreessche, J. Watmough, Reproduction numbers and sub-threshold endemic equilibria for compartmental models of disease transmission, *Math. Biosci.*, **180** (2022), 29–48. [https://doi.org/10.1016/S0025-5564\(02\)00108-6](https://doi.org/10.1016/S0025-5564(02)00108-6)
31. H. R. Thieme, Spectral bound and reproduction number for infinite dimensional population structure and time heterogeneity, *SIAM J. Appl. Math.*, **70** (2009), 188–211. <https://doi.org/10.1137/080732870>

32. A. Cintrón-Arias, C. Castillo-Chávez, L. M. A. Bettencourt, A. L. Lloyd, H. T. Banks, The estimation of the effective reproductive number from disease outbreak data, *Math. Biosci. Eng.*, **6** (2009), 261–282. <https://doi.org/10.3934/mbe.2009.6.261>
33. H. Haario, M. Laine, A. Mira, E. Saksman, DRAM: efficient adaptive MCMC, *Stat. Comput.*, **16** (2006), 339–354. <https://doi.org/10.1007/s11222-006-9438-0>
34. M. D. McKay, R. J. Beckman, W. J. Conover, A comparison of three methods for selecting values of input variables in the analysis of output from a computer code, *Technometrics*, **21** (1979), 239–245. <https://doi.org/10.1080/00401706.2000.10485979>
35. *Guidelines for Organization of Regional Novel Coronavirus Nucleic Acid Tests (Third Edition) (in Chinese)*, 2022. Available from: <http://www.nhc.gov.cn/yzygj/s7659/202203/b5aaa96dfe1b4f14b19bf2f888a10673.shtml>.
36. J. Qi, D. Zhang, X. Zhang, T. Takana, Y. Pan, P. Yin, et al., Short- and medium-term impacts of strict anti-contagion policies on non-COVID-19 mortality in China, *Nat. Hum. Behav.*, **6** (2022), 55–63. <https://doi.org/10.1038/s41562-021-01189-3>



AIMS Press

©2023 the Author(s), licensee AIMS Press. This is an open access article distributed under the terms of the Creative Commons Attribution License (<http://creativecommons.org/licenses/by/4.0>)